Published in Surface Science 331-333, issue 1, 80-87, 1995
which should be used for any reference to this work

Direct structural information from X-ray photoelectron diffraction: intermixing and on-surface adsorption of Na on Al surfaces

R. Fasel *, P. Aebi, J. Osterwalder, L. Schlapbach

Institut de Physique, Université de Fribourg, 1700 Fribourg, Switzerland

Abstract

We have investigated the local structures of the room-temperature Na adsorption phases on Al(001) and (111) surfaces with X-ray photoelectron diffraction. Angular distributions of X-ray excited Na 1s photoelectrons and Na KVV Auger electrons emitted from c(2 × 2)-Na/Al(001), ($\sqrt{3} \times \sqrt{3}$)R30°-Na/Al(111) and p(2 × 2)-Na/Al(111) have been measured over the full solid angle above the Al surfaces. We show that angle-scanned photoelectron diffraction, in contrast to other structural techniques, gives very direct information on the degree of intermixing at the surface. Many structural models can be ruled out directly from the experimental results, and for the case of intermixing the interface structure can be determined by simple geometrical considerations.

Keywords: Alkali metals; Aluminum; Low index single crystal surfaces; Photoelectron diffraction; Physical adsorption; Surface relaxation and reconstruction; Surface structure

1. Introduction

Due to the chemical selectivity and the sensitivity to local order X-ray photoelectron diffraction is a powerful technique for surface structural investigations [1]. The dominant effects determining the photoelectron angular distribution from a given structure are different depending on the kinetic energy regime of the electrons (Fig. 1a). At energies above 500 eV the strong anisotropy in the individual electron–atom scattering leads to a forward focusing of electron flux along directions pointing from the photoemitter to the scatterer. The analysis of the symmetry and positions of forward-focusing maxima thus permits a very straightforward identification of *bond directions* and structural symmetry. Below about 200 eV the scattering becomes more isotropic, and interferences between different scattering paths prevail. Due to the axial symmetry of each emitter–scatterer pair, constructive interferences of an unscattered and a singly scattered wave can be recognized in the diffraction pattern as concentric circular fringes centered at the corresponding forward-focusing directions. As the phase condition for constructive interference depends on the emitter–scatterer distance d, the opening half angle θ of an interference fringe contains the *bond length* information:

$$kd(1 - \cos\theta) + \psi(\theta) = 2\pi n. \quad (1)$$

* Corresponding author. E-mail: roman.fasel@unifr.ch.

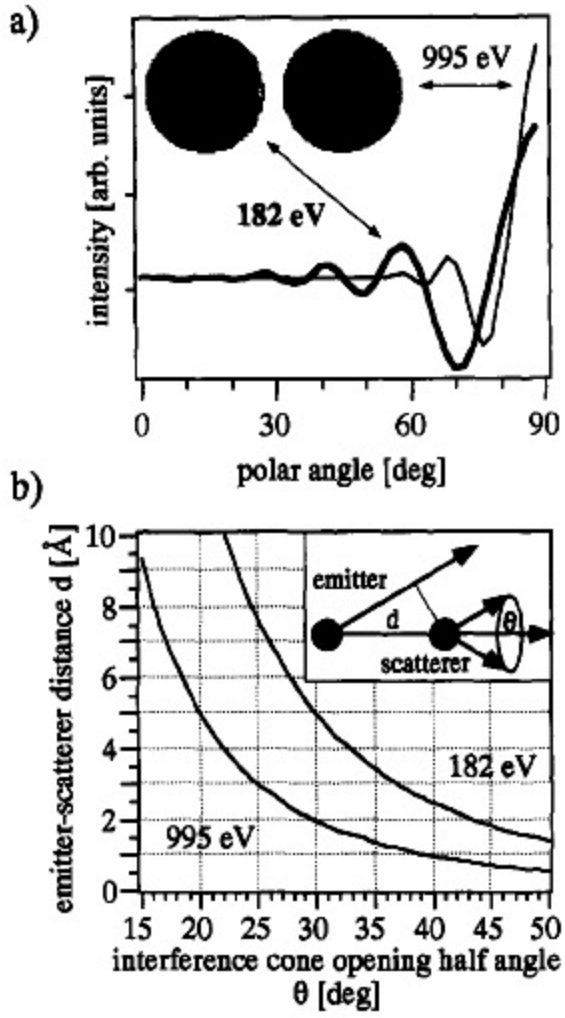

Fig. 1. (a) Polar-angle photoelectron intensity distribution for a dimer of two Na atoms, calculated for kinetic energies of 182 and 995 eV, respectively, within the single scattering approximation. The inset shows the corresponding full hemispheric intensity distributions in stereographic projection. At 182 eV, the first-order interference fringe can clearly be recognized. (b) Correspondence between first-order interference cone opening half angle θ and emitter–scatterer distance d for a Na scatterer calculated using Eq. (1).

Here k is the wave number, $\psi(\theta)$ is the scattering phase shift, and n is the order of interference. The correspondence between the angle θ and the emitter–scatterer distance d is shown in Fig. 1b for the case of scattering from a Na atom for the energies corresponding to Na 1s (Mg K α) and Na KVV electrons.

The combination of high and low energy XPD patterns should thus allow the determination of bond directions and bond lengths in a very direct way through identification of forward focusing directions and determination of the interference cone opening angles. In the following we apply this approach to three different Na on Al systems.

2. Na adsorption on Al surfaces

In contradiction to the "traditional" expectation that the alkali atoms adsorb in the most highly coordinated position on a practically undisturbed surface, it has been shown by high-resolution core-level spectroscopy that the room temperature (RT) adsorption of Na, K, Rb and Cs on Al(111), as well as the adsorption of Na on Al(001), lead to a disruption of the Al surface and to the formation of a surface alloy [2]. For c(2 × 2)-Na/Al(001), a recent surface extended X-ray absorption fine structure (SEXAFS) study proposed Na adsorption beneath a reconstructed surface Al layer [3], whereas very recent investigations using density functional theory conclude that for the RT c(2 × 2)-Na/Al(001) system the adsorption energy of the hollow site is the lowest for very low coverages and that at a coverage of about 0.15 ML a transition from hollow to substitutional site occupation should occur [4].

For $(\sqrt{3} \times \sqrt{3})$R30°-Na/Al(111) it has been shown by SEXAFS [5] and normal incidence standing X-ray wavefield absorption (NISXW) [6] that the Na atoms adsorb in substitutional sites, thus kicking out every third surface Al atom. From a NISXW study of the p(2 × 2)-Na/Al(111) phase a model involving two reconstructed layers each of stoichiometry $NaAl_2$ was proposed [7]. Other structures suggested for this phase are a distorted double layer of bcc Na(111) lattice planes [8], and a three domain model with a p(2 × 1) periodicity [9]. There is thus a high degree of controversy as to the structure of these three phases.

3. Experimental

The experiments were performed in a modified Vacuum Generators ESCALAB Mark II spectrome-

ter equipped with a three-channeltron detection system and with a base pressure in the lower 10^{-11} mbar region. Photoelectron spectra and diffraction patterns were measured at RT using Mg Kα ($h\nu$ = 1253.6 eV) radiation. Contamination free surfaces as judged by photoemission were achieved by a combination of Ar^+ sputtering and annealing at 500° C. Na was evaporated from carefully outgassed SAES getter sources. The purity of the deposited Na layers as well as the coverage were checked by core-level photoemission. The samples were then in situ transferred to a two-axis goniometer capable of sweeping the photoelectron emission direction over the whole hemisphere above the surface by computer controlled crystal rotation. Using a fast data acquisition mode without background subtraction [10] allowed us to use a high sampling density (6000 angles) while keeping the scan times reasonably short

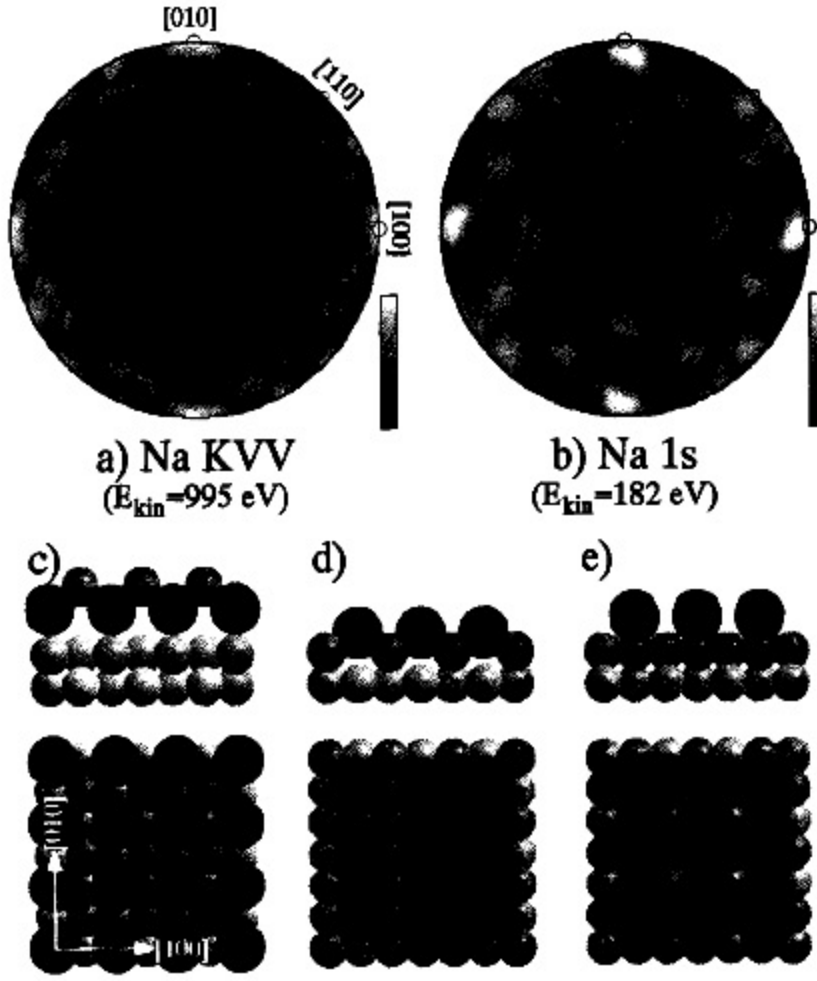

Fig. 2. Experimental XPD patterns from the RT c(2 × 2)-Na/Al(001) structure: (a) Na KVV at 995 eV kinetic energy, and (b) Na 1s at 182 eV kinetic energy. The data have been stereographically projected and normalized according to the procedure described in the text. Forward scattering directions and corresponding interference fringes are indicated in the patterns. Front and top views of Na (black) on Al(001) adsorption geometries. (c) The subsurface alloy geometry proposed in Ref. [3]. (d) The substitutional geometry, where every second surface Al atom has been kicked out and replaced by a Na atom. (e) The hollow site geometry.

(< 5 h). Under these conditions the oxygen and carbon contaminations were always maintained below 0.1 ML.

4. Experimental results and discussion

4.1. Weakly intermixed systems: c(2 × 2)-Na / Al(001) and (√3 × √3)R30°-Na / Al(111)

The measured diffraction patterns of the Na KVV peak at 995 eV and the Na 1s peak at 182 eV kinetic energy are shown in Figs. 2 and 3 for c(2 × 2)-Na/Al(001) and (√3 × √3)R30°-Na/Al(111), respectively. To maximize the statistical accuracy the patterns have been azimuthally averaged exploiting the 4-fold and 3-fold rotational symmetries of the systems. To eliminate the smooth polar angle dependence of the photoelectron intensity typical for adsorbate emission, the patterns have been normalized with respect to the mean intensity for each polar emission angle. Both effects discussed in Section 1 are clearly visible in these measured patterns. The prominent features of the Na KVV as well as of the Na 1s diffraction patterns are strong forward focusing maxima in the surface plane and circular fringes around these [11]. From the absence of forward focusing peaks at non-grazing angles it follows immediately that for both structures there are no atoms situated above the Na atoms. The subsurface model

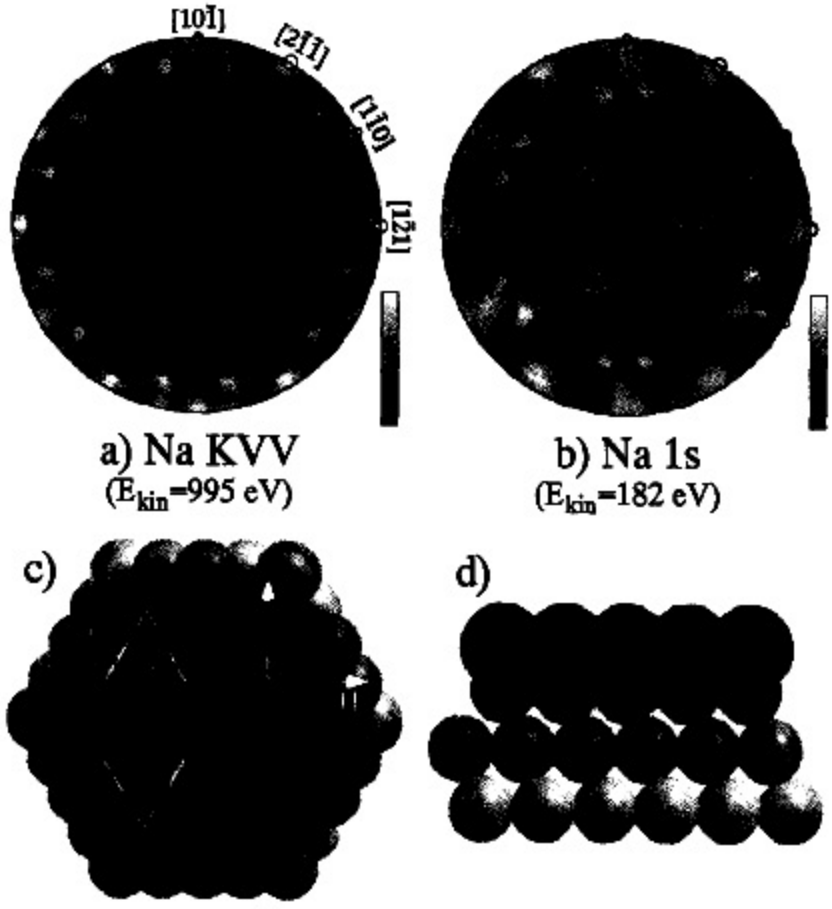

Fig. 3. Experimental XPD patterns from the RT (√3 × √3)R30°-Na/Al(111) structure: (a) Na KVV at 995 eV kinetic energy, and (b) Na 1s at 182 eV kinetic energy. The data have been stereographically projected and normalized according to the procedure described in the text. Forward scattering directions and corresponding interference fringes are indicated in the patterns. (c) Top and (d) front views of the substitutional (√3 × √3)R30°-Na (black) on Al(111) adsorption geometry.

Table 1
Quantitative results from the geometrical analysis of the c(2 × 2)-Na/Al(001) and ($\sqrt{3}$ × $\sqrt{3}$)R30°-Na/Al(111) diffraction patterns

Structure	Symmetry	NN directions	θ_{NN}	NN distance (Å)	NNN directions	θ_{NNN}	NNN distance (Å)
c(2 × 2)-Na/Al(001)	4	⟨100⟩	33 ± 1°	4.0 ± 0.3	⟨110⟩	28.5 ± 1°	5.6 ± 0.5
($\sqrt{3}$ × $\sqrt{3}$)R30°-Na/Al(111)	6	⟨1$\bar{2}$1⟩	30.5 ± 1°	4.8 ± 0.4	⟨1$\bar{1}$0⟩	23 ± 1°	9.2 ± 0.9

The in-plane NN and NNN distances are calculated from the respective interference cone opening half angles θ_{NN} and θ_{NNN} (Eq. (1)).

for the c(2 × 2)-Na/Al(001) structure proposed by Aminpirooz et al. [3] and depicted in Fig. 2c can thus definitely be ruled out.

From the positions of the forward focusing peaks in the Na KVV diffraction patterns the directions of the in-plane neighbours of the Na emitters can be

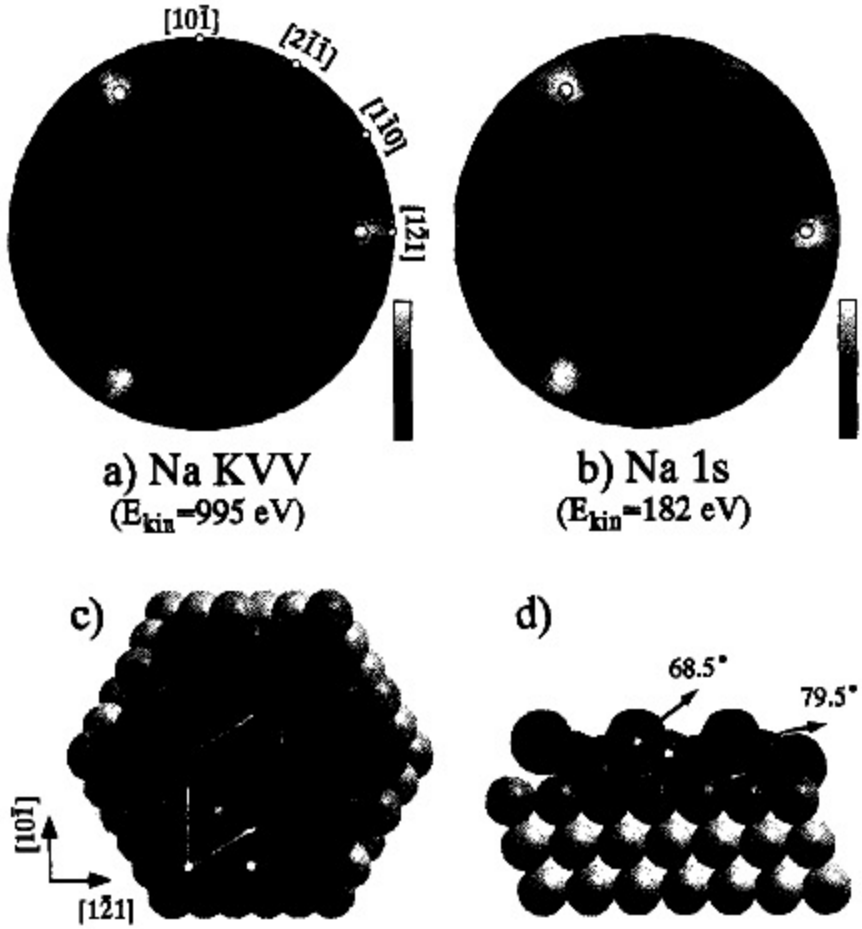

Fig. 4. Experimental XPD patterns from the RT p(2 × 2)-Na/Al(111) structure: (a) Na KVV at 995 eV kinetic energy, and (b) Na 1s at 182 eV kinetic energy. The data have been stereographically projected and normalized according to the procedure described in the text. Forward scattering directions and corresponding interference fringes are indicated in the patterns. (c) Top and (d) front views of the proposed surface structure of p(2 × 2)-Na (black) on Al(111). The interatomic directions accounting for the forward scattering peaks indicated in (a) and (b) are marked by arrows.

determined. Nearest neighbours (NN) and next-nearest neighbours (NNN) can furthermore be distinguished by the opening angle of the corresponding first-order interference fringes in the Na 1s patterns (Fig. 1b, Eq. (1)). The results from this simple geometrical analysis of the c(2 × 2)-Na/Al(001) and ($\sqrt{3} \times \sqrt{3}$)R30°-Na/Al(111) diffraction patterns are summarized in Table 1, and the positions of nearest and next-nearest in-plane neighbours as well as the corresponding interference fringes are indicated in Figs. 2 and 3. The experimentally determined NN distances of $d_{\langle 100 \rangle} = 4.0 \pm 0.3$ Å and $d_{\langle 1\bar{2}1 \rangle} = 4.8 \pm 0.4$ Å correspond to the bond distances associated with a c(2 × 2) Na nearest neighbour on Al(001) (4.05 Å) and a ($\sqrt{3} \times \sqrt{3}$)R30°-Na nearest neighbour on Al(111) (4.96 Å), respectively. As the NN distances for an in-plane substitutional site would be considerably shorter (2.86 Å for both surfaces) and furthermore be oriented along the $\langle 110 \rangle$ and $\langle 1\bar{1}0 \rangle$ directions, respectively, we can conclude that the Na atoms are definitely not coplanar with the top Al layer but must be considerably moved out of this plane.

By the simple analysis given above we have shown that the two structures – c(2 × 2)-Na/Al(001) and ($\sqrt{3} \times \sqrt{3}$)R30°-Na/Al(111) – consist of pure Na surface layers with no coplanar Al atoms, adsorbed above the top Al substrate layers. The only way to reconcile this with the core level spectra of Andersen et al. [2] giving evidence for some kind of "intermixing" is thus that the Na atoms occupy substitutional sites while showing a considerable outward buckling. For ($\sqrt{3} \times \sqrt{3}$)R30°-Na/Al(111) substitutional adsorption has been confirmed by SEXAFS [5] and NISXW [6]. For c(2 × 2)-Na/Al(001) we have performed a detailed study involving single scattering cluster (SSC) calculations and an *R*-factor analysis to determine the exact adsorption site of the Na atoms [12]. Our results indicate that the RT c(2 × 2)-Na/Al(001) structure consists of coexisting domains of Na atoms adsorbed in the substitutional and in the hollow sites (Figs. 2d, 2e), with Na–Al bond lengths of 3.11 and 2.93 Å, respectively. This unusual and unexpected behaviour can be understood in the light of very recent theoretical results from density-functional theory [4]. For ($\sqrt{3} \times \sqrt{3}$)R30°-Na/Al(111) a detailed study is currently under way.

4.2. A strongly intermixed system: p(2 × 2)-Na/Al(111)

The measured diffraction patterns of the Na KVV peak at 995 eV and the Na 1s peak at 182 eV kinetic energy are shown in Fig. 4. Again, the patterns have been azimuthally averaged exploiting the 3-fold rotational symmetry of the system and normalized with respect to the mean intensity for each polar emission angle. From the Na KVV diffraction pattern it is immediately evident that the p(2 × 2)-Na/Al(111) structure involves a much stronger intermixing than the lower coverage ($\sqrt{3} \times \sqrt{3}$)R30° structure. The appearance of six strong forward focusing peaks at non-grazing emission angles excludes all two-dimensional models, and in particular the model proposed in Ref. [9] consisting of three domains with p(2 × 1) periodicity each. On the other hand the absence of forward focusing peaks at small emission angles excludes all models containing atoms on top of Na atoms. The model involving two reconstructed layers of stoichiometry $NaAl_2$ proposed in Ref. [7] contains Al atoms atop second-layer Na atoms, and it can thus be ruled out. The double layer model of distorted bcc Na(111) planes [8] cannot account for the two inequivalent forward scattering directions seen in the Na KVV diffraction pattern.

The Na coverage of the p(2 × 2) structure is 0.5 ML, and the unit cell thus contains 2 Na atoms. Considering this fact, the structure of the p(2 × 2)-Na/Al(111) phase can be readily determined from the positions of the forward scattering peaks in the Na KVV diffraction pattern, which appear at polar emission angles of 79.5 ± 1° in the $\langle 1\bar{2}1 \rangle$ azimuths and at 68.5 ± 1° in the $\langle 2\bar{1}\bar{1} \rangle$ azimuths. As there are two and only two Na atoms per p(2 × 2) unit cell, the two inequivalent forward focusing directions cannot be explained by Na scattering only, but one additional Al atom has to be involved. The construction of the model is now as follows: As a starting point, we substitute every fourth surface Al atom by a Na atom, thus forming a p(2 × 2) superstructure. We now have to place two additional atoms in the unit cell – one Na atom and one Al atom – at polar angles of 79.5° and 68.5° from the substitutional Na atom to account for the two inequivalent forward focusing directions. There are two high symmetry sites per unit cell with respect to the underlying Al

substrate and the p(2 × 2) Na superstructure, which are the 3-fold coordinated fcc and hcp adsorption sites of the fcc (111) surface. Placing the atoms into these sites and considering the observed polar angles, vertical positions above the substitutional Na atoms are 1.3 ± 0.1 and 0.6 ± 0.1 Å for the atoms in the fcc and hcp adsorption sites, respectively. If the atom adsorbed in the hcp site would be a Na atom, the Al atom in the hcp site 0.7 Å above would give rise to a forward focusing peak at about 67° in the $\langle 1\bar{2}1 \rangle$ azimuths, which is not observed. We can thus assign the Na atom to the fcc site and the Al atom to the hcp site. If we assume for the substitutional Na atoms the same Na–Al bond length of 3.3 Å as determined for the substitutional Na atoms of the $(\sqrt{3} \times \sqrt{3})$R30° structure [5], we obtain bond lengths of 3.4 and 2.8 Å for the Na atoms in the fcc sites and the Al atoms in the hcp sites, respectively. The value of 2.8 Å for the Al atoms in the hcp site is very close to the bulk value of 2.86 Å for pure Al, and the bond length of 3.4 Å for the fcc Na atoms is reasonably close to the one of the substitutional Na atoms.

The model of the p(2 × 2)-Na/Al(111) structure derived above is shown in Figs. 4c and 4d. The interatomic directions corresponding to the forward focusing peaks in the Na KVV diffraction pattern of Fig. 4a are indicated by arrows. As an independent test of the structural model and to determine the atomic positions to a higher degree of precision we have performed SSC calculations and a *R*-factor analysis for both the Na 1s and the Na KVV diffraction patterns. The detailed results of this analysis will be presented elsewhere [13], and we only mention here that it fully confirms the structural model derived above.

5. Conclusions

By considering full hemispherical X-ray photoelectron diffraction measurements of the RT c(2 × 2)-Na/Al(001), $(\sqrt{3} \times \sqrt{3})$R30°-Na/Al(111) and p(2 × 2)-Na/Al(111) structures, we have shown that angle-scanned photoelectron diffraction gives very direct information on the degree of intermixing at the surface. Taking two diffraction patterns of the same structure, one at 995 eV and one at 182 eV, bond directions as well as approximate bond lengths could be readily determined. Many structural models proposed in the literature could be ruled out directly, and for the case of p(2 × 2)-Na/Al(111) the interface structure could be determined by simple geometrical considerations. We find that the p(2 × 2) unit cell of this structure consists of one Na atom substituting a surface Al atom, an additional Na atom in the fcc adsorption site and one Al atom in the hcp adsorption site.

Acknowledgements

We thank C. Stampfl for useful discussions and for communicating results prior to publication. Skillful technical assistance was provided by E. Mooser, O. Raetzo and H. Tschopp. This project has been supported by the Fonds National Suisse pour la Recherche Scientifique.

References

[1] For a review see: C.S. Fadley, in: Synchrotron Radiation Research: Advances in Surface Science, Ed. R.Z. Bachrach (Plenum, New York, 1990).
[2] J.N. Andersen, E. Lundgren, R. Nyholm and M. Qvarford, Surf. Sci. 289 (1993) 307.
[3] S. Aminpirooz, A. Schmalz, L. Becker, N. Pangher, J. Haase, M.M. Nielsen, D.R. Batchelor, E. Bøgh and D.L. Adams, Phys. Rev. B 46 (1992) 15594.
[4] C. Stampfl, J. Neugebauer and M. Scheffler, Surf. Rev. Lett. 1 (1994) 22.
[5] A. Schmalz, S. Aminpirooz, L. Becker, J. Haase, J. Neugebauer, M. Scheffler, D.R. Batchelor, D.L. Adams and E. Bøgh, Phys. Rev. Lett. 67 (1991) 2163.
[6] M. Kerkar, D. Fisher, D.P. Woodruff, R.G. Jones, R.D. Diehl and B. Cowie, Phys. Rev. Lett. 68 (1992) 3204.
[7] M. Kerkar, D. Fisher, D.P. Woodruff, R.G. Jones, R.D. Diehl and B. Cowie, Surf. Sci. 278 (1992) 246.
[8] A. Hohlfeld and K. Horn, Surf. Sci. 211/212 (1989) 844.
[9] J.O. Porteus, Surf. Sci. 41 (1974) 515.
[10] More details about the data acquisition procedure for obtaining 2π intensity maps can be found in Ref. [12].
[11] The patterns for $(\sqrt{3} \times \sqrt{3})$R30°-Na/Al(111) contain some faint structure associated with emission from the Al substrate. At the time these measurements were performed, the Mg anode used was slightly Si contaminated. The Al struc-

ture seen in the patterns is due to Si Kα excited Al electrons emerging at the same energy as the Mg Kα excited Na electrons. We have checked that the only features introduced by this are the 3 mutually crossing dark lines in the Na KVV pattern ($\langle 101 \rangle$ planes) and the 3 broad maxima at the crossing points of these lines in the Na 1s pattern ($\langle 101 \rangle$ directions).

[12] R. Fasel, P. Aebi, J. Osterwalder, L. Schlapbach, R.G. Agostino and G. Chiarello, Phys. Rev. B 50 (1994) 14516.

[13] R. Fasel, P. Aebi, J. Osterwalder and L. Schlapbach, in preparation.